Wind and Structures, *Vol. 18, No. 1 (2014) 057-067*
DOI: http://dx.doi.org/10.12989/was.2014.18.1.057

The inertial coefficient for fluctuating flow through a dominant opening in a building

Haiwei Xu*, Shice Yu and Wenjuan Lou

College of Civil Engineering and Architecture, Zhejiang University, Hangzhou, 310058, China

(Received April 10, 2013, Revised August 20, 2013, Accepted September 5, 2013)

Abstract. For a building with a dominant windward wall opening, the wind-induced internal pressure response can be described by a second-order non-linear differential equation. However, there are two ill-defined parameters in the governing equation: the inertial coefficient C_I and the loss coefficient C_L. Lack of knowledge of these two parameters restricts the practical use of the governing equation. This study was primarily focused on finding an accurate reference value for C_I, and the paper presents a systematic investigation of the factors influencing the inertial coefficient for a wind-tunnel model building including: opening configuration and location, wind speed and direction, approaching flow turbulence, the model material, and the installation method. A numerical model was used to simulate the volume deformation under internal pressure, and to predict the bulk modulus of an experimental model. In considering the structural flexibility, an alternative approach was proposed to ensure accurate internal volume distortions, so that similarity of internal pressure responses between model-scale and full-scale building was maintained. The research showed 0.8 to be a reasonable standard value for the inertial coefficient.

Keywords: wind tunnel test; dominant opening; internal pressure; inertial coefficient; Helmholtz resonance

1. Introduction

The occasional opening or failure of doors and windows during severe wind events may create a dominant opening in a building, and generate internal pressure fluctuations, which, when combined with external pressures, can cause damage to a roof and building envelope. Therefore, an appropriate estimate of peak internal pressure is essential for building design, especially given the growing number of low-rise and large-span buildings in typhoon-prone areas. By introducing the Helmholtz resonator model, Holmes (1979) innovatively described the response of the internal pressure to wind action with a second-order non-linear differential equation. Liu and Saathoff (1981, 1982), Vickery *et al.* (1986, 1992), and Sharma and Richards (1997a, b) proposed alternative versions of the internal pressure governing equation. However, there are two uncertain parameters C_I, C_L therein: C_I is an inertial coefficient defining the effective length of an oscillating air slug at the opening by $l_e = l_0 + C_I\sqrt{A_0}$. The loss coefficient C_L represents frictional, expansion, contraction, and miscellaneous energy losses. Although wind tunnel investigations (Oh *et al*. 2007,

*Corresponding author, Dr., E-mail: haiwe163@163.com

http://www.techno-press.org/?journal=was&subpage=8 ISSN: 1226-6116 (Print), 1598-6225 (Online)

Ginger *et al*. 2010) and TTU full-scale field measurement (Ginger *et al*. 1997, 1999) have corroborated the finding that the non-linear governing equation is able to predict internal pressure responses with suitable values of C_I and C_L, the exact values of the two parameters remain uncertain. Regarding the governing equation, one of the main arguments lies in whether or not flow contraction occurs at opening. Liu *et al*. (1982) and Sharma *et al*. (1997a, b) observed a region of convergent flow forming when the air jet entered through opening, while Vickery *et al*. (1986, 1992) argued that flow contraction does not occur in unsteady flow. As a result, two different forms of the Helmholtz frequency equation are presented

$$f_H = \frac{1}{2\pi}\sqrt{\frac{\gamma A_0 P_a}{\rho_a V_0 (l_0 + C_I\sqrt{A_0})}} \tag{1}$$

$$f_H = \frac{1}{2\pi}\sqrt{\frac{c\gamma A_0 P_a}{\rho_a V_0 (l_0 + C_I\sqrt{A_0})}} \tag{2}$$

ρ_a, P_a are the density and pressure of the air respectively, γ is the specific heat ratio, A_0 is the opening size, V_0 is internal volume of the model, l_0 is physical length of the orifice, and c represents a flow coefficient. Comparison of Eqs. (1) and (2) show that C_I in Eq. (1) is essentially equivalent to C_I/c in Eq. (2). To assess the inertial coefficients on an equal basis, data for C_I based on Eq. (2) have already been divided by c in this paper and values of C_I discussed subsequently are all based on Eq. (1).

Liu and Saathoff (1981) suggested that 1.33 is probably the correct value for C_I. According to potential flow theory, Vickery *et al.* (1992) gave a theoretical C_I = 0.89 for sharp-edged circular openings. Sharma *et al*. (1997b) defined the parameter by opening location and the ratio of the physical opening length l_0 to the effective radius $r = \sqrt{A_0/\pi}$. For a long opening (l_0/r>1.0), C_I = 0.98, but for thin openings (l_0/r < 1.0), C_I varies with opening location, from 1.3 (opening near the centre of the wall) to between 1.1 and 1.22 (opening adjacent to the floor). Ginger *et al*. (1997, 2010) and Holmes (1979) both agreed that $C_I = \sqrt{\pi/4}$. By fitting the best coefficients to match the measured data for a single opening model, Yu *et al.* (2006) obtained a value of C_I of around 1.3.

To apply this internal pressure governing equation to building design, two ill-defined parameters must be evaluated. The parametric study in this paper is based on the governing equation of Holmes (1979) shown in Eq. (3) and its un-damped Helmholtz resonant frequency is given by Eq. (1).

$$\frac{\rho_a (l_0 + C_I\sqrt{A_0})V_0}{\gamma A_0 P_a}\ddot{C}_{pi} + C_L\frac{\rho_a V_0^2 q}{2\gamma^2 A_0^2 P_a^2}\dot{C}_{pi}\left|\dot{C}_{pi}\right| + C_{pi} = C_{pe} \tag{3}$$

In Eq. (3), C_{pi} and C_{pe} are internal and external pressure coefficients respectively. As far as model flexibility is concerned, an effective volume $V_e = V_0 \times (1 + K_a/K_b)$ (K_a is the bulk modulus of air and K_b is the bulk modulus of the building) will be used instead of V_0. Holmes (2007) pointed out that the recommended values of K_a/K_b for typical low-rise buildings lie between 0.2 to 5. $q = 1/2\rho_a U_h^2$ is the reference dynamic pressure at roof height, and U_h is the mean wind speed at roof height.

Using dimensional analysis, Holmes (1979) showed that Eq. (3) could also be expressed as a

function of several non-dimensional parameters: $\Phi_1 = A_0^{3/2}/V_0$, $\Phi_2 = \alpha_s/U_h$, $\Phi_3 = \rho_a U_h\sqrt{A_0}/\mu$, $\Phi_4 = \sigma_U/U$, $\Phi_5 = \lambda/\sqrt{A_0}$, $S^* = \Phi_1\Phi_2^2$, and $t^* = tU_h/\lambda$. α_s is the speed of sound, λ is the integral length scale of the turbulence, and t^* is non-dimensional time, μ is the dynamic viscosity of air, U and σ_u are the mean and root-mean-square wind speed, respectively. Then Eq. (3) can be rewritten in the dimensionless form

$$\frac{C_I}{S^*\Phi_5^2}\frac{d^2C_{pi}}{dt^{*2}} + \frac{C_L}{4S^*\Phi_5}\frac{dC_{pi}}{dt^*}\left|\frac{dC_{pi}}{dt^*}\right| + C_{pi} = C_{pe} \tag{4}$$

Eq. (4) indicates that the internal pressure fluctuations are closely related to parameters C_I, C_L, S^*, and Φ_5. Although slight differences exist in the value of inertial coefficient due to the influence of multiple factors, previous studies showed that there may be a common value for C_I. This paper is mainly concerned with finding an appropriate value of the inertial coefficient in model scale, and the factors influencing it, including: the opening configuration and position, wind speed and direction, the turbulence intensity in the incoming flow, the building model material, and the installation method of a wind-tunnel model.

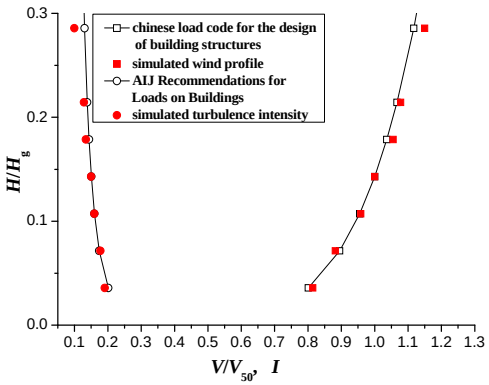

Fig. 1 Profile of simulated mean wind velocity and turbulence intensity along with codes

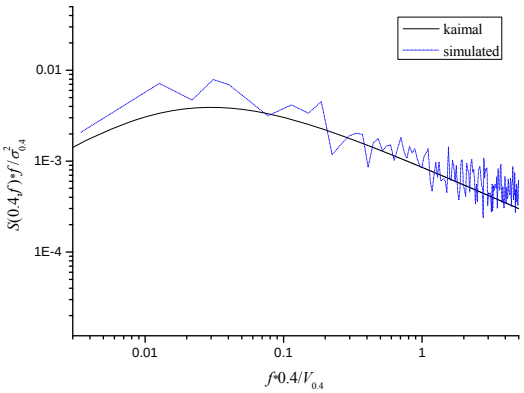

Fig. 2 Spectrum of fluctuating wind velocity at 0.4 m height with target Kaimal spectrum

2. Wind tunnel investigations

2.1 Experiment details

Models made from steel, Perspex®, and Acrylonitrile Butadiene Styrene (ABS) were tested in the wind tunnel in Zhejiang University. A 1:250 scale boundary layer representing Terrain Category B in the Chinese load code for the design of building structures (2002) was simulated in the wind tunnel. The mean wind velocity and turbulence intensity along with the code provisions (2002, 2004) are plotted in Fig. 1 where H_g is the gradient height of the boundary layer and V_{50} represents the wind velocity at 50 cm height (model scale) or 125 m height (full scale), I is the turbulence intensity. The non-dimensional longitudinal velocity spectrum measured at 0.4 m height

exhibits reasonable agreement with the target Kaimal spectrum in Fig. 2. $V_{0.4}$ and $\sigma_{0.4}$ are mean and RMS wind speed at 0.4 m height in the wind tunnel respectively. The mean wind speed at roof height was 12.8 ms^{-1} and the pressure signals from each tap were sampled at 625 Hz for 32 s. For each material, various opening configurations were adopted during the experiments. Assuming the model was rigid, the inertial coefficient C_I can be determined from the measured Helmholtz frequency using Eq. (1). For rigid models, these recognised C_I values can be regarded as realistic. For flexible models, the directly identified inertial coefficients are essentially nominal values encompassing the effects of material flexibility, and can be converted to real values by considering the influence of effective volume.

2.2 Steel model

A fully-rigid model with dimensions of 25 cm (W) × 25 cm (L) × 10 cm (H) was welded together using steel plates approximately 1 cm thick. In this case, wind induced internal volume change could be ignored and the parameter C_I obtained can be assumed to be reliable. For this model, 10 different central opening configurations were tested at mean wind velocities at roof height of 12.8 ms^{-1} and 7.5 ms^{-1} respectively to study the effect of opening configuration and wind velocity. For C_I = 0.8, the theoretically predicted and the experimentally-identified Helmholtz frequencies are listed in Table 1.

Table 1 Predicted and measured Helmholtz frequencies for 10 opening configurations

test case	velocity (m/s)	height or diameter(mm)	width (mm)	depth (mm)	theoretical f_h(Hz)	measured f_h(Hz)	absolute errors(%)
1	12.8	35.3	35.3	3.9	136.6	136.9	0.2
2	7.5	35.3	35.3	3.9	136.6	136.8	0.1
3	12.8	43.3	28.8	3.9	136.6	136.9	0.2
4	7.5	43.3	28.8	3.9	136.6	136.6	0.0
5	12.8	50	24.9	3.9	136.5	135.9	0.4
6	7.5	50	24.9	3.9	136.5	136.8	0.2
7	12.8	29.8		3.3	117.2	118	0.7
8	7.5	29.8		3.3	117.2	117.1	0.1
9	12.8	39.9		4.4	135.6	135.6	0.0
10	7.5	39.9		4.4	135.6	136	0.3
11	12.8	49.8		5.5	151.5	150	1.0
12	7.5	49.8		5.5	151.5	149.5	1.3
13	12.8	69.8		6.8	180.8	179.7	0.6
14	7.5	69.8		6.8	180.8	180.2	0.3
15	12.8	40		9.5	126.3	131.6	4.2
16	7.5	40		9.5	126.3	132	4.5
17	12.8	39.8		19.5	112.0	116	3.6
18	7.5	39.8		19.5	112.0	114.9	2.6
19	12.8	40		40	94.0	93.5	0.5
20	7.5	40		40	94.0	95.8	1.9

Table 1 shows that the absolute errors between the predicted and measured f_h are all below 5%;

therefore $C_I = 0.8$ appears to be satisfactory for all tested cases. Furthermore, it is apparent that the inertial coefficient is not sensitive to changes in wind speed and opening configuration. As far as the Helmholtz frequency of Eq. (1) is concerned, 0.8 appears to be an accurate value of C_I.

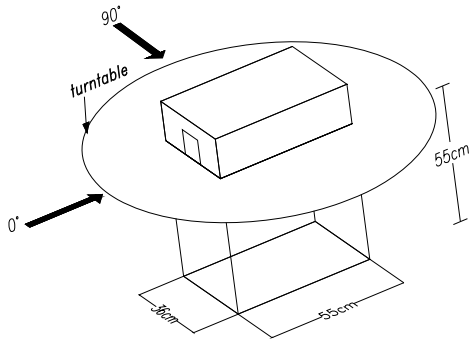

Fig. 3 Sketch of Perspex® model

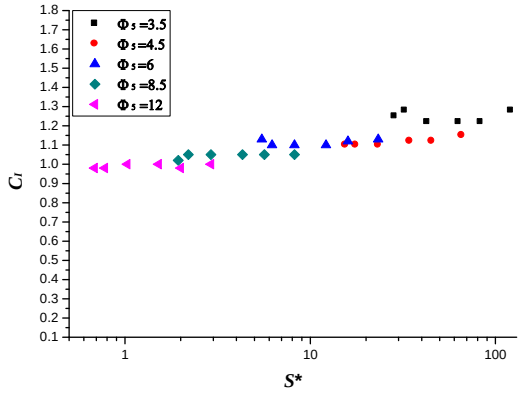

Fig. 4 Inertial coefficient C_I *versus* S^*

2.3 Perspex® model

In fact, steel is rarely used in normal wind tunnel tests because of its heavy weight. For comparison purpose, the widely-used flexible material Perspex® was chosen to build a 36.4 cm (W) × 54.8 cm (L) × 16 cm (H) model (shown in Fig. 3). Five opening configurations comprising: A1 (30 cm (W) × 10 cm (H)), A2 (20 cm (W) × 10 cm (H)), A3 (10 cm (W) × 10 cm (H)), A4 (5 cm (W) × 10 cm (H)), A5 (5 cm (W) × 5 cm (H)) could be separately installed in the middle of the bottom of the 364 mm long windward wall. A 55 cm (L) × 36 cm (W) × 55 cm (H) adjustable chamber located under the turntable provided additional internal volume for the model. For each opening size, the internal pressure was measured for: V_0, $1.5V_0$, $2V_0$, $3V_0$, $4V_0$, and $4.5V_0$ (V_0 = 36.4 cm × 54.8 cm × 16 cm) at incident wind directions of 0° to 90°. Variation of C_I with S^* is illustrated in Fig. 4. Most measured inertial coefficients lay between 1.0 and 1.3 which matches the

recommendation of Sharma (1997a, b). The values also remain practically unchanged with increasing S^* for a given Φ_5. Furthermore, the parameter also tends to increase with the opening area. For the central opening cases A2~A5, there is a slight difference in inertial coefficient values which mainly concentrate in the range of 1-1.1. However, the lst opening A1 is approximately as wide as windward wall and opening porosity is 55%, therefore the air slug oscillation is less effected by opening windward wall and the excitation energy is increased, which may lead to larger inertial coefficient. Since the opening A1 does not satisfy basic characteristics of typical small dominant opening models, it will not be discussed in the following parametric study. The C_I for this model is actually the nominal value involving amplification by the multiplier $(1 + K_A/K_B)$, and flexible materials increase the multiplier; this explains why Perspex® models produce larger C_I values than steel ones.

To examine the influence of opening location, turbulence intensity, and wind direction, models with internal volume V_0 were selected for further study. Turbulence intensities of 16 % and 20 % at roof height and opening locations 1 to 4 (as shown in Fig. 5) were investigated. Identified C_I values are listed in Tables 2 and 3. It seems that the turbulence intensity of incoming flow and opening locations have limited impact on the parameter. Similarly, the variation of C_I with wind azimuths as plotted in Fig. 6 indicates the inertial coefficient is nearly independent of wind direction.

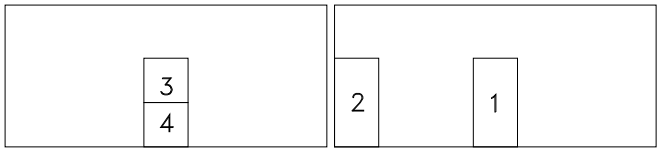

Fig. 5 Sketch of opening location in windward wall

Table 2 C_I for model with volume V_0 in different turbulence intensities

opening area	low turbulence	high turbulence
A2	1.1	1.12
A3	1.1	1.04
A4	1.05	1.01
A5	1.0	0.98

Table 3 C_I for different opening locations

opening location	1	2	3	4
C_I	1.05	1.1	1.08	1.02

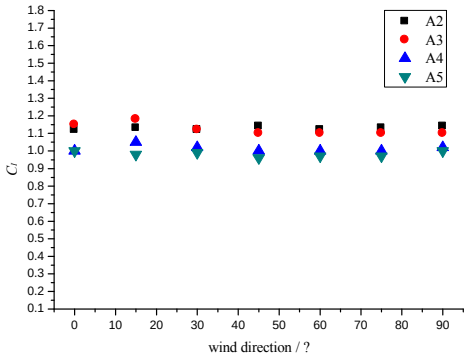

Fig. 6 Variation of C_I with wind direction

2.4 ABS model

Considering the importance of material flexibility on the outcome of nominal C_I values, models made from ABS, with an elastic modulus lower than the previous two model materials, were subsequently tested. Nominal C_I values for a 0.566 m^3 model with 0.083 m^2 or 0.025 m^2 windward wall openings are 1.5 and 1.4 respectively, both of which exceed the maximum values from steel and Perspex® models. Therefore the more flexible the material is, the larger the nominal inertial coefficient will be.

2.5 Influence of model installation

Generally, influence factors can be divided into two aspects: physical characteristics of the model such as: its installation method, material flexibility, opening configuration, internal volume, *etc*., and external excitation characteristics such as the wind conditions. Most of these factors have been discussed above, except for model installation approaches which will be discussed in this section.

Two types of installation method were used. Initially the model was fixed to the wind tunnel turntable with adhesive tape. Then the connections between the model and turntable were augmented by four angle steels. C_I values for the two cases are listed in Table 4 which reveals that the inertial coefficient decreases as the connection stiffness (which restrained the models' deformations under internal pressure) increases.

Table 4 C_I for different installation methods

installation method	$A_0(m^2)$	$V_0(m^3)$	C_I
adhesive tape	0.0038	0.0065	1.4
adhesive tape + angle steels	0.0038	0.0065	1.1

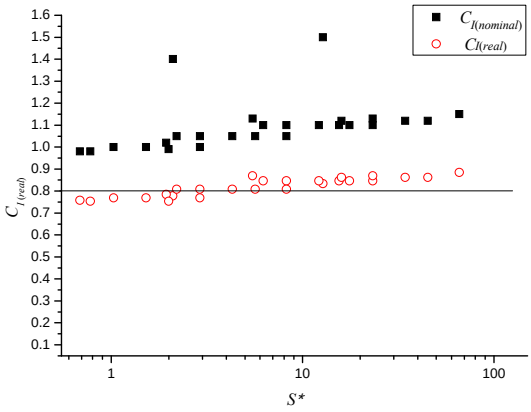

Fig. 7 C_I values for non-rigid models

3. Verification of the standard value for C_I

As discussed earlier, the inertial coefficient of a flexible model, with and without regard to the effective volume, can be denoted by $C_{I(real)}$ and $C_{I(nominal)}$, respectively. If the proposed standard value is reasonable, whatever material a model is made of, $C_{I(real)}$ should be around 0.8. To derive $C_{I(real)}$ for a flexible model, the amplification factor $(1 + K_a/K_b)$ must be determined. According to Vickery *et al*. (1992), K_a is equal to γP_a and the effective volume depends on bulk modulus K_b which is difficult to measure in the experiment. Hence finite element analysis software (ANSYS) was used to simulate the internal volume change ($\triangle V_0$) to unit pressure and K_b was obtained by solving for $V_0/\triangle V_0$. To accurately reflect the material characteristics and working conditions of the models, the displacements of roofs and wall centres of the numerical models were calibrated against the experimental model under the same concentrated force. If the simulated K_b is assumed to be accurate, $C_{I(real)}$ exclusive of material flexibility's influence can be defined as the identified $C_{I(nominal)}$ divided by $(1 + K_a/K_b)$. The simulation results of K_a/K_b values for ABS and *Perspex*® models are 0.8 and 0.3 respectively, and the corresponding $C_{I(real)}$ values are plotted in Fig. 7, showing that most of $C_{I(real)}$ values are lower than those directly recognized $C_{I(nominal)}$ and approaching the standard one(0.8). However, for some cases (such as *Perspex*® model with opening A2), the simulated $C_{I(real)}$ is still slightly larger than the standard one. This may possibly be attributed to two factors: one is that the test models were generally assembled by connecting separate plates with adhesive or bolts and the model's structural integrity was therefore reduced, whereas the numerical model used rigid connections. This may have lead to smaller change in the internal volume of the numerical model compared to those in the actual one under the same pressure. The other reason is that the model constraints at floor level are too complicated to be precisely simulated by this numerical model, which will give rise to differences between sets of results. These reasons will eventually result in a more conservative K_a/K_b ratio and hence a larger $C_{I(real)}$ relative to the standard value. In spite of that, the simulation results justify the choice of 0.8 as an appropriate standard value for the inertial coefficient. In addition, Fig. 7 also implies that the internal volume change for flexible models cannot be ignored in a wind tunnel test. In other words,

for non-rigid models those directly identified inertial coefficients are invalid, unless the effect of material deformation is eliminated.

4. Application of the standard value in internal volume distortion

To maintain dynamic similarity, the internal pressure fluctuations inside a model should satisfy

$$\frac{\lambda_l \lambda_V}{\lambda_A \lambda_t^2} \frac{\rho l_e V_0}{\gamma A P_a} \ddot{C}_{pi} + \frac{\lambda_V{}^2 \lambda_u{}^2}{\lambda_A{}^2 \lambda_t^2} \frac{C_L \rho V_0^2 q}{2\gamma^2 A^2 P_a^2} \cdot \dot{C}_{pi} \left| \dot{C}_{pi} \right| + C_{pi} = C_{pe} \tag{5}$$

where λ_l, λ_A, λ_V, λ_t, and λ_u are the ratio of length, area, volume, and time between model and full-scale building, respectively. $\lambda_A=\lambda_l^2$, $\lambda_t=\lambda_l/\lambda_u$.

Applying similarity theory gives

$$\frac{\lambda_l \lambda_V}{\lambda_A \lambda_t^2} = \frac{\lambda_V{}^2 \lambda_u{}^2}{\lambda_A{}^2 \lambda_t^2} = 1 \tag{6}$$

Simplifying Eq. (6) gives

$$\lambda_V = \frac{\lambda_l^3}{\lambda_u{}^2} \tag{7}$$

Considering material flexibility and substituting $V_e= V_0\times(1+K_a/K_b)$ into Eq. (7) yields

$$V_m = \frac{V_f \times \lambda_l^3}{\lambda_u{}^2} \times \frac{1+(K_{af}/K_{bf})}{1+(K_{am}/K_{bm})} \tag{8}$$

Subscripts f and m represent full- and model-scale respectively. Eq. (8) shows that internal volume distortion is a function of bulk modulus and wind velocity ratio. When $K_{bf} = K_{bm}$, the internal volume of a model need to be exaggerated by the square of the full-scale to model velocity ratio just as Holmes (1979) recommended and no additional volume distortion will be required, if the result of $\dfrac{1+(K_{af}/K_{bf})}{1+(K_{am}/K_{bm})}$ happens to be $\lambda_u{}^2$. Actually, it is somewhat inconvenient to directly use Eq. (8) due to uncertainties in bulk modulus K_{bm}. Consequently, an alternative method is presented to obtain the correct internal volume distortion as follows

i) With an accurate blueprint or a suitably refined numerical model, K_{bf} for a full-scale building can be more easily and precisely simulated by numerical method than K_{bm}.

ii) Full-scale Helmholtz frequency can be calculated from Eq. (1) with C_I = 0.8. Then, according to frequency ratio λ_f ($\lambda_f = f_{Hm} / f_{Hf}$) which can be found by solving λ_u/λ_l , the Helmholtz frequency of the model can be derived.

iii) Varying the internal volume continuously until the Helmholtz frequency converges to the desired value derived in last step.

As an example, a full-scale building with a dominant opening was used to assess the efficacy of the method. Salient parameters were as follows: A_{0f} = 1250 m^2; V_{0f} = 505960 m^3; K_{af}/K_{bf} = 0.4; λ_u = 0.5; λ_l = 1/250; λ_f = 125; f_{Hf} = 0.43 Hz; and f_{Hm} = 53.5 Hz. An internal volume V_m of 0.113 m^3 was observed in a wind-tunnel test when f_{Hm} reached 53 Hz. Analytical full-scale internal pressure

spectrum along with its measured model-scale counterpart is plotted in Fig.8. z and V_z represent roof height and mean wind speed at roof level respectively, while σ_p is equal to $0.5\rho_a V_z^2$. Fig. 8 shows favourable agreement between resonance frequencies and peaks of the two spectra; this verifies the efficacy of the proposed volume distortion method.

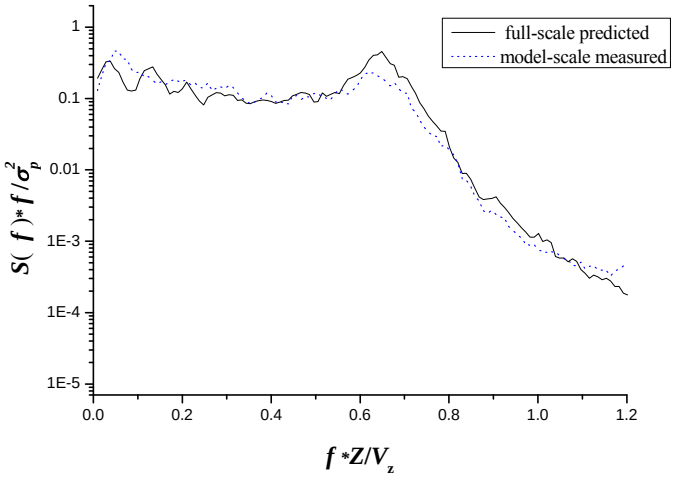

Fig. 8 Non-dimensional internal pressure power spectrum

5. Conclusions

A series of wind tunnel tests were carried out on models made from different materials to determine an accurate value for the inertial coefficient C_I. Experimental and numerical analysis were combined to study those factors possibly influencing this key parameter. The main conclusions are listed below:

- The study implies that 0.8 is a convincing reference value for inertial coefficient C_I.
- The influence of opening configuration and location, wind speed and direction, and turbulence intensity on C_I is insignificant. Fixity between the model and the wind tunnel's turntable upon which it is mounted is required to obtain reliable values of C_I.
- $C_{I(nominal)}$ increases as the material stiffness decreases. Internal volume change caused by a model's flexibility should not be neglected. Although numerical simulation can be adopted to predict the bulk modulus of a model so that $C_{I(nominal)}$ can be corrected to $C_{I(real)}$, inaccurate $C_{I(real)}$ values may arise due to an insufficiently refined numerical model. To avoid this problem, materials with a high stiffness but a low density are the preferred option for such wind tunnel tests.
- An effective method is proposed to achieve the prospective internal volume in order to maintain dynamic similarity of internal pressure. If the internal volume cannot be distorted under experimental conditions, the material for the test model should be chosen properly so as to make the value of $\dfrac{1+(K_{af}/K_{bf})}{1+(K_{am}/K_{bm})}$ tend to λ_u^2 as far as is possible.

References

Architectural Institute of Japan (2004), AIJ recommendations for loads on buildings, Tokyo.

China Academy of Building Research (2002), Load code for the design of building structures, China.

Ginger, J.D., Mehta, K.C. and Yeatts, B.B. (1997), "Internal pressures in a low-rise full-scale building", *J. Wind. Eng. Ind. Aerod*.,**72** ,163-174.

Ginger, J.D., Letchford, C.W (1999), "Net pressure on low-rise full-scale building", *J. Struct. Eng - ASCE*., **83**(1-3), 239-250.

Ginger, J.D., Holmes, J.D. and Kim, P.Y. (2010), "Variation of internal pressure with varying sizes of dominant openings and volumes", *J. Struct. Eng - ASCE*., **136**(10), 1319-1326.

Holmes, J.D. (1979), "Mean and fluctuating pressures induced by wind", *Proceedings of the 5th International Conference on Wind Engineering***,** Fort Collins, Colorado, USA.

Holmes, J.D. (2007), *Wind loading of structures* (2nd Ed.), Taylor &Francis Group.

Liu, H. and Saathoff, P.J. (1982), "Internal pressure and building safety", *J. Struct. Eng - ASCE*., **108**(10), 2223-2234.

Liu, H. and Saathoff, P.J (1981), "Building internal pressure: sudden change", *J. Eng. Mech. Div*., **107**(2),109-321.

Oh, H.J., Kopp, G.A. and Inculet, D.R. (2007), "The UWO contribution to the NIST aerodynamic database for wind load on low buildings: Part 3.Internal pressure", *J. Wind. Eng. Ind. Aerod*., **95**(8),755-779.

Sharma, R.N. and Richards, P.J. (1997a), "Computational modeling of the transient response of building internal pressure to a sudden opening", *J. Wind. Eng. Ind. Aerod*.,**72**, 149-161.

Sharma, R.N. and Richards, P.J. (1997b), "Computational modeling in the prediction of building internal pressure gain function", *J. Wind. Eng. Ind. Aerod*. **67-68**, 815-825.

Vickery, B.J (1986), "Gust factors for internal pressures in low-rise buildings", *J. Wind. Eng. Ind. Aerod*., **23**, 259-271.

Vickery, B.J. and Bloxham, C. (1992), "Internal pressure dynamics with a dominant opening", *J. Wind. Eng. Ind. Aerod*., **41**,193-204.

Yu, S.C., Lou, W.J. and Sun, B.N. (2006), "Wind-induced internal pressure fluctuations of structure with single windward wall opening", *J. Zhejiang Univ. Sci.- A*, **7**,415-423.

JH